UNCLASSIFIED

SECURITY CLASSIFICATION OF THIS PAGE (When Data Entered)

AD-A244 276

N PAGE

READ INSTRUCTIONS BEFORE COMPLETING FORM

2. GOVT ACCESSION NO. N/A

3. RECIPIENT'S CATALOG NUMBER N/A

(2)

Electro-optic Generation and Detection of Femtosecond Electromagnetic Pulses

5. TYPE OF REPORT & PERIOD COVERED Final 1 Aug 88 - 30 Sep 91

6. PERFORMING ORG. REPORT NUMBER

7. AUTHOR(s) David H. Auston

8. CONTRACT OR GRANT NUMBER(s) F49620-88-C-0109

AFOSR-TR- 92 0017

9. PERFORMING ORGANIZATION NAME AND ADDRESS
Columbia University
Department of Electrical Engineering
New York, NY 10027

10. PROGRAM ELEMENT, PROJECT, TASK AREA & WORK UNIT NUMBERS 2301/A1

11. CONTROLLING OFFICE NAME AND ADDRESS
U. S. Army Research Office
Post Office Box 12211
Research Triangle Park, NC 27709

12. REPORT DATE November 20, 1991

13. NUMBER OF PAGES 29

14. MONITORING AGENCY NAME & ADDRESS(if different from Controlling Office)
AFOSR
H. Schlossberg
Bolling Air Force Base, DC 20332-6448

15. SECURITY CLASS. (of this report) Unclassified

15a. DECLASSIFICATION/DOWNGRADING SCHEDULE

16. DISTRIBUTION STATEMENT (of this Report)

Approved for public release; distribution unlimited.

DTIC ELECTE JAN 14 1992 S D

17. DISTRIBUTION STATEMENT (of the abstract entered in Block 20, if different from Report)

NA

18. SUPPLEMENTARY NOTES

The view, opinions, and/or findings contained in this report are those of the author(s) and should not be construed as an official Department of the Army position, policy, or decision, unless so designated by other documentation.

19. KEY WORDS (Continue on reverse side if necessary and identify by block number)

N/A

20. ABSTRACT (Continue on reverse side if necessary and identify by block number)

See attached report, page 2.

92-01110

DD FORM 1 JAN 73 1473 EDITION OF 1 NOV 65 IS OBSOLETE

UNCLASSIFIED

SECURITY CLASSIFICATION OF THIS PAGE (When Data Entered)

92 1 13 028

ELECTRO-OPTIC GENERATION and DETECTION of FEMTOSECOND ELECTROMAGNETIC PULSES

David H. Auston
Department of Electrical Engineering
Columbia University
New York, NY 10027

FINAL REPORT
Contract #F49620-88-C-0109
Submitted to H. Schlossberg
Air Force Office of Scientific Research
Bolling Air Force Base
DC 20332-6448

ABSTRACT

This final technical report summarizes research activities during the period August 1, 1988 to September 30 1991 under contract #F49620-88-C-0109, "Electro-optic Generation and Detection of Femtosecond Electromagnetic Pulses". Key accomplishments during this period are: [1] The successful demonstration of a new technique for generating sub-picosecond electromagnetic pulses using large aperture photoconductors to produce directional and diffraction-limited beams of terahertz radiation; [2] The development of a new electrically-controlled phased array of photoconducting antennas for producing steerable terahertz radiation; [3] The extraction of femtosecond electromagnetic pulses from an electro-optic crystal following their generation by electro-optic Cherenkov radiation, and their subsequent propagation and detection in free space; [4] The measurement of subpicosecond electrical response of a new organic electro-optic material (polymer); [5] The observation of terahertz transition radiation from the surfaces of electro-optic crystals.

CONTENTS:

A. RESEARCH OBJECTIVES.

The following objectives were stated in the original contract with regard to research on the electro-optic generation and detection of femtosecond electromagnetic pulses:

[1] To explore the use of new electro-optic materials in addition to lithium tantalate.

[2] To devise techniques for coupling the Cherenkov radiation cone out of the crystals.

[3] To extend the technology to low temperature environments.

[4] To generate high amplitude electric field pulses.

[5] To explore new applications for materials measurements.

B. SUMMARY

The accomplishments obtained in the pursuit of the planned research objectives in the period of August 1, 1988 to September 30, 1991 are as follows: [1] We have successfully demonstrated a new technique for generating subpicosecond electromagnetic pulses using large aperture photoconductors to produce directional and diffraction-limited beams of terahertz radiation. The direction of the terahertz radiation can be optically-controlled by changing the incident angle of the optical beam. A study of the power scaling properties suggests that scaling to MegaWatt peak powers is possible in aperture up to 25 cm^2. We have also tested a large variety of semiconductors as the photoconductors to optimize the radiation. [2] The development of a new electrically-controlled phased array of photoconducting antennas for producing steerable terahertz radiation. This device allows us to steer the terahertz radiation by varying the spatial distribution of the bias voltage across the array. [3] The development of a new optoelectronic technique to characterize the surface and interface electronic properties of semiconductors through the measurement of the surface field by optically induced femtosecond

electromagnetic radiation. This technique can be used for the measurement of the amplitude and direction of the surface static field, doping type and dopant concentration, transient carrier mobility, and even crystal symmetry. [4] The extraction of femtosecond electromagnetic pulses from an electro-optic crystal ($LiTaO_3$) following their generation by electro-optic Cherenkov radiation, and their subsequent propagation and detection in free space. [5] The measurement of subpicosecond electrical response of a new organic electro-optic material (polymer). A 760 femtosecond risetime electrical transient (corresponding to a bandwidth of 460 GHz) is observed from a poled side chain polymer film via electrooptic sampling technique. [6] The observation of terahertz transition radiation from the surfaces of the electro-optic crystals.

C. STATUS OF THE RESEARCH EFFORT.

1. New Materials and Techniques.

Substantial progress has been made in the area of the investigation of new materials and techniques for generating and detecting femtosecond electromagnetic pulses. Work in these areas will be summarized under the following headings:

a. Organic Electro-optic Materials.

We have investigated the electrical transient response of an organic electro-optic polymer for the detection of ultrafast electrical pulses. This is the continuation of the research with Drs. James Yardley and Paul Ferm of the Allied Signal Corporation to investigate the properties of new organic electro-optic materials. Measurements have been made of the ultrafast electro-optic response through electro-optic polymer films. These films, which were prepared at Allied Signal, were the copolymer of 60% methylmethacrylate (MMA) and 40% methacrylate-bound disperse red 1 dye (MA1). We used the standard elecro-optic sampling technique to measure the transient response of the polymer film. A GaAs photoconductor which connects with a coplanar transmission line was used to generate a electrical transient with a risetime comparable with the optical excitation pulse duration. A poled polymer film was placed on the top of the transmission lines which has a 20 mm line width

and gap space between the lines. The electrical signal was measured through the birefringence change of the polymer film while an electrical transient propagates above the film. Both reflection and transmission geometries for the detection were used in the sampling technique. We have measured the femtosecond electro-optic response and sensitivity of these poled side chain polymer films; a 760 femtosecond risetime electrical transient has been observed by using electro-optic sampling techniques. This ultrafast transient demonstrated the viability of these polymer films for use in ultrafast devices with bandwidth beyond 400 GHz. The measured 760 femtosecond risetime is currently limited by the device structure which uses 20 μm wide transmission lines. Due to the fact that the hyperpolarizability in a polymer film mainly from an electronic origin rather than from an ionic origin, a faster electrical response is expected by using an optimized structure.

We have also measured the second order nonlinear coefficient r_{33}. A value r_{33} of 14 pm/volt has been found in our electro-optic polymer, this value is about half of that from a $LiTaO_3$ crystal.

The main interest in polymers as an electro-optic probe material will be to take advantage of their other material properties. Low dielectric constant will cause less loading of the transmission line. Submicron to micron thicknesses allow for shorter optical transit times. By minimizing the interaction time between the electrical transient and optical pulse, the transient can be recorded with finer temporal resolution.

b. Electro-optic Transition Radiation.

We have observed transition radiation from the surfaces of the electro-optic materials by using femtosecond laser pulses. The time-resolved far infrared radiation signal clearly indicated that this radiation comes from the interface between the electro-optic material and the air.

This process is analogous to the classical concept of the radiation that occurs when a charged particle (electric monopole) passes through the interface separating one dielectric medium from another. In the case of electro-optic materials, the passage of an optical pulse from one dielectric medium to another also generates a low frequency radiation that appears to

emanate from the interface. The physical mechanism, however, is simply the same as the bulk optical rectification effect, except that the lack of perfect phase-matching causes the signal from the bulk to cancel, leaving only contributions from the regions within a coherence length of the entrance and exit faces. The effect differs from the previously studied electro-optic Cherenkov radiation, in that it does not require tight focussing of the optical beam, and so can be used with higher optical fluxes.Cherenkov radiation which is mainly a bulk effect, an electro-optic transition radiation generated by a laser beam (not tightly focused) through an electro-optic crystal is emitted only within a coherence length near the surface. . In our experiments, we have observed electro-optic transition radiation from several electro-optic materials, including $LiTaO_3$, $LiNbO_3$ and KDP crystals. The radiation was detected by a photoconducting dipole detector.

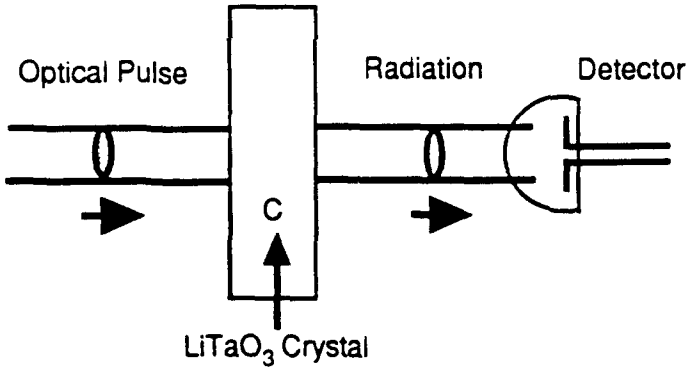

Fig. 1: Experimental setup for transition radiation.

Figure 1 schematically illustrates experimental setup. A short laser pulse has a normal incident angle on a thin electro-optic slab of thickness L.

The nonlinear rectified polarization induced by a laser pulse inside the electro-optic media is

$$P_k^{NL}(r,t) = -\frac{\varepsilon_0}{4} n_0^4 \sum_{i,j} r_{ijk} E_i(r,t) E_j^*(r,t) \qquad (1)$$

where n_0 is the optical index of refraction of the laser and E_i is the complex electric field of the laser pulse.The radiation field E due to the rectification

from an electric dipole satisfies a nonlinear wave equation (the laser pulse propagates in the x direction):

$$\frac{\partial^2 E}{\partial x^2} - \frac{\varepsilon_s}{c^2}\frac{\partial^2 E}{\partial t^2} = \frac{\partial^2 P^{NL}}{\partial t^2} \tag{2}$$

where we assume: i) the laser beam size is large enough that we can use the plane wave approximation; ii) the rectification polarization P^{NL} is perpendicular to x and has a value described by equation (1) ($P \neq 0$ for $0<x<L$ and $P^{NL}=0$ otherwise); iii) by using ε_s, the static dielectric constant of the media, the dispersion of the radiation field is ignored. With the considerations of absorption of the radiation field inside the electro-optic slab and small reflection of the radiation on the surfaces, we find the solution of equation (2) at the region x>L:

$$E(x,t) = \frac{\frac{c_0}{v}+\frac{c_0}{c}}{1+\frac{c_0}{v}} P^{NL}\left(t-\frac{x-L}{c_0}-\frac{L}{c}\right) - \frac{2\frac{c_0}{v}\left(1+\frac{c_0}{c}\right)}{\left(1+\frac{c_0}{v}\right)^2} P^{NL}\left(t-\frac{x-L}{c_0}-\frac{L}{v}\right)$$
$$+\frac{\left(1-\frac{c_0}{v}\right)\left(1-\frac{c_0}{c}\right)}{1+\frac{c_0}{v}} P^{NL}\left(t-\frac{x-L}{c_0}-\frac{L}{c}-\frac{2L}{v}\right)+\cdots \tag{3}$$

where c_0, c, and v are the speed of the laser beam in the air, in the medium, and the speed of radiation beam in the medium, respectively. The first term of the left side in equation (3) is the transition radiation at the interface x=L; the second term is the radiation at the interface x=0; and the rest of the terms are the multi-reflections of the transition radiation inside the slab or the transition radiation due to the multi-reflection of the optical pulse inside the slab. The common feature of each term is that they share the same temporal shape as the rectification dipole P^{NL} or the optical intensity of the laser pulse; so, the radiation pulse duration should be the same as the optical pulse if the dispersion effect can be ignored. This is actually true for the radiation at x=L, i. e. the first term in equation (3); but not quite accurate for the radiation from x=0, because the dispersion of the radiation signal is not small and absorption of the radiation is strong in the medium. These effects attenuate and distort the radiated pulse which emanates from

the entrance face and propagates through the crystal. Another feature of the radiated signals is that the sign of the radiated field from the x=0 interface is opposite to the field from the x=L interface, and the time delay between the two signals is equal to the travelling time delay between the radiation pulse and the optical pulse passing through the crystal (L/v-L/c).

Figure 1 schematically illustrates the experimental setup. A colliding pulse mode-locking (CPM) laser was used as the femtosecond optical source. The laser has 60 fs pulse duration with 100 MHz repetition rate, 620 nm wavelength and 20 mW average power. Several $LiNbO_3$ and $LiTaO_3$ crystals with their thickness ranging from 0.15 mm to 1 mm were studied. A lens with 15 cm focus length was used to focus the CPM beam down to 1 mm diameter on the slab. The incident angle of laser beam was normal and the polarization of the laser beam was along the crystal c-axis. The detector was a 100-μm dipole antenna with the radiation-damaged Si-on-Sapphire as the photoconductor. The detector, which placed 10 mm behind the slab, was gated by the split optical pulse at a time delay. The temporal measurement was achieved by varying the time delay between the excited laser pulse and the gated laser pulse. The gated signal from the photoconducting antenna was amplified, averaged, and digitized by a current amplifier, a lock-in amplifier, and a computer.

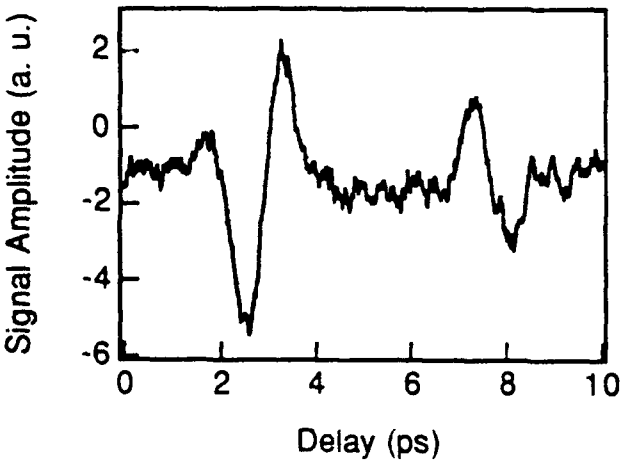

Fig. 2: Electro-optic transition radiation from a 0.5 mm thick $LiNbO_3$ crystal.

Figure 2 shows the temporal waveform of the transition radiation from a 0.5 mm thick $LiNbO_3$. Two pulses with opposite polarity are the radiated field at two surfaces; the pulse with a short time is the radiation from the surface x=L and the pulse with a long time is the radiation from x=0. Because of the

microwave attenuation in the crystal, the radiation from x=0 has a smaller amplitude. The measured pulse width is the convolution of the radiation field with the detector response. Since the detector has a 0.5 ps response time, the actual waveform is broadened by the detector. The time separation between the two pulses is about 5 ps. This time delay is close to the calculated value of 5.3 ps (the difference of the travelling time between the optical signal and the radiation signal passing through the 0.5 mm $LiNbO_3$ slab). Similar measurements have also been performed in the $LiTaO_3$. Figure 3 shows the waveform of the transition radiation from a 0.22 mm thick $LiTaO_3$ sample. The measured delay time of approximately 3 ps agrees with the calculated delay time of 3.2 ps. The good agreement between the measured data and calculated result is evidence that the radiation pulses came from the two interfaces between the crystal and the air. Due to the larger $\varepsilon_s(\varepsilon_3)$ of $LiTaO_3$, than that of $LiNbO_3$, the radiation signal from $LiTaO_3$ is smaller. The calculated radiation field from the $LiTaO_3$ by using a CPM laser is about 0.2 V/cm. By using an amplified CPM laser with microjoule pulse energy, the radiation field could be as high as many kV/cm.

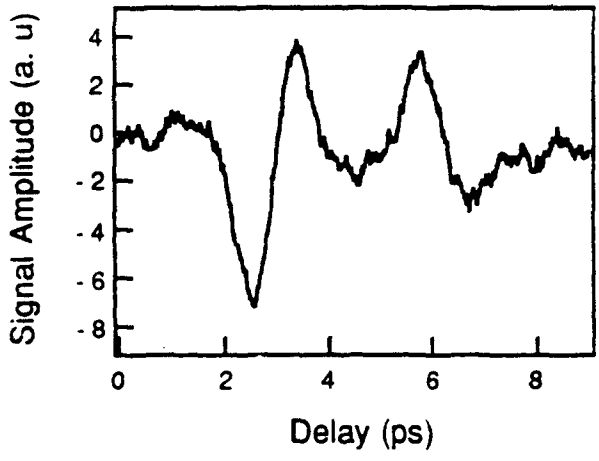

Fig. 3: Electro-optic transition radiation from a 0.22 mm thick $LiTaO_3$ crystal.

2. Generation and Detection of THz Electromagnetic Pulses.

In previous years, we demonstrated the basic principal and properties of these devices, including their directionality and steerable features. This year, our research has concentrated on the following three new aspects: (1) an investigation of saturation properties of different materials; (2) extensive research of photoconducting antenna array for generating terahertz beams (the beam can be electronically steered and the center frequency of the

radiation can be electronically selected); and, (3) transient carrier dynamics with the injected photocarrier energy around the band edge.

a. Saturation Properties of Different Materials.

We have measured the radiated electric field as a function of optical excitation fluence in large-aperture antennas consisting of different photoconductors. These experiments were performed on InP, GaAs and RDSOS samples with a 0.5 mm spacing of photoconductor gap and a bias electric field, E_b, of 4000 V/cm.

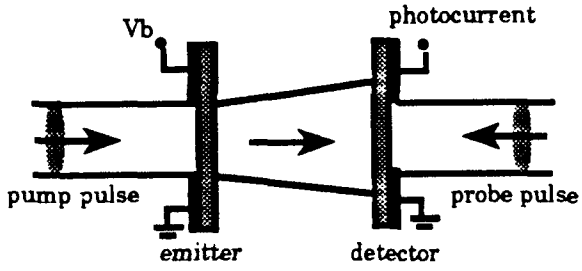

Fig. 4: Generation and detection of femtosecond electromagnetic pulses by large-aperture photoconducting antennas

The experimental apparatus is shown in Figure 4. The large-aperture emitter is illuminated at normal incidence. The emitting antennas consist of a planar photoconductor with a pair of parallel aluminum electrodes. The large-aperture detector is placed directly in front of the emitter at a distance much larger than the dimensions of this antenna (i. e. in the far field region). This device is similar in structure to the emitter but in some cases the gap spacings between the respective pairs of electrodes may differ. The large-aperture detector consists of a photoconductor of a short carrier lifetime to provide adequate time resolution. No optical components are used to image the radiation to the detector so that an absolute measurement of the radiated field could be obtained. Optical pulses used in our experiments were derived from a balanced colliding-pulse, mode-locked ring dye laser amplified by a copper vapor laser pumped amplifier. The detector was a large-aperture antenna incorporating an epilayer of low temperature MBE grown GaAs (LT GaAs). This photoconductor was grown at 200 ^{o}C to a thickness of 2 μm. The parallel electrodes consist of a gold germanium alloy annealed to the surface intended to provide an Ohmic contact. The gap spacing between the

electrodes in this particular structure was 0.5 mm. LT GaAs has been shown to have a carrier lifetime of approximately 200 fs. A dipole antenna consisting of this material has previously been used to detect terahertz radiation.

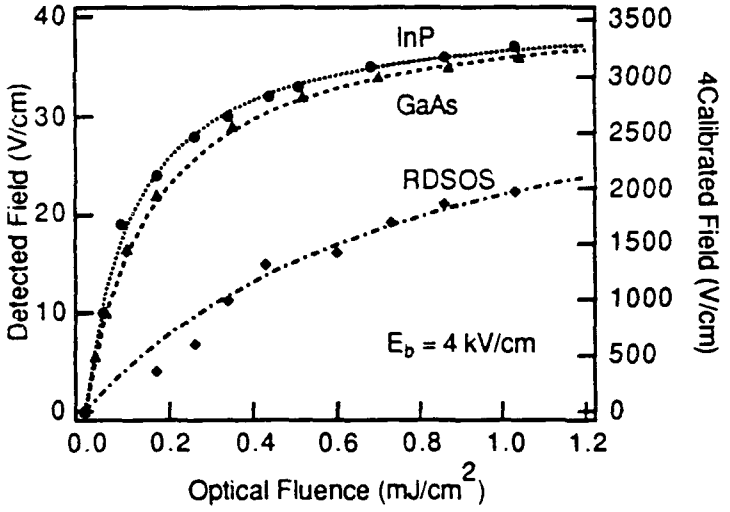

Fig. 5: Saturation curves of photoconductors with different materials

Figure 5 shows radiation field from different photoconductors vs optical fluence. The depicted points represent experimental data and the dashed lines are the plots from the calculation. A value for E_b of 3600 V/cm was used in the calculations of the three curves in Figure 5. This value is slightly less than the value of experimentally applied field of 4000 V/cm. One of the possible reasons for this discrepancy is the voltage drop near the contact of the electrodes on the sample and absorption of the emitted radiation in the substrates of the antennas.

In Figure 5, strong saturation was observed in both InP and GaAs. A transient carrier mobility of 300 cm^2/V-s and 220 cm^2/V-s is measured for InP and GaAs. These electron mobilities are much less than those of the steady state values of 4600 cm^2/V-s and 8500 cm^2/V-s for InP and GaAs, respectively. The primary reason for this is that the carriers are not in thermal equilibrium with respect to the lattice of the photoconductor in the first few picoseconds after excitation by an optical pulse of photon energy much larger than the band gap.

Because of the relatively low electron mobility, the saturation in the radiation-damaged silicon-on-sapphire (RDSOS) large-aperture antenna was not as significant as in the previous two materials. The radiated field from the RDSOS device is sublinear with respect to optical excitation fluence. The theoretical curve assumes an electron mobility of 30 $cm^2/V\text{-}s$ comparable to the measured value of 29 $cm^2/V\text{-}s$.

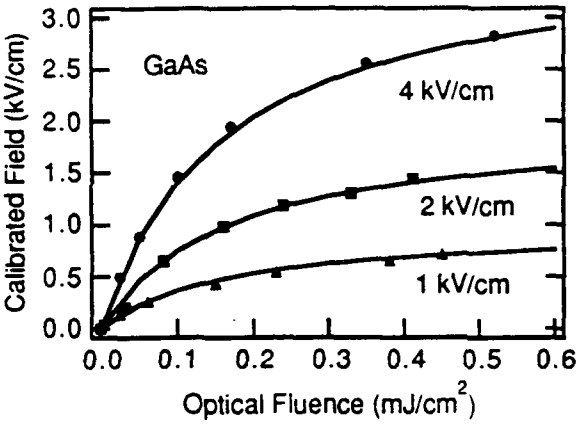

Fig. 6: Radiation field as a function of optical fluence with three bias fields.

Figure 6 shows the calibrated field as a function of optical fluence in a 0.5 mm gap GaAs antenna for 1000 V/cm, 2000 V/cm and 4000 V/cm. In this figure, the shapes refer to the experimental data and the lines are the best fit. The emitters used in this experiment were subject to damage at 1 mJ/cm^2 optical excitation fluence for electric fields exceeding 5000 V/cm. This corresponded to electrical heating on the order of 50 - 100 mW partially caused by the dark conductivity. This thermal problem can readily be avoided by the application of a pulsed bias with a low duty cycle and or the excitation by an optical source with a lower duty cycle than the one used here.

b Electrically Steerable Photoconducting Antenna Arrays.

In previous years, we have shown that the large aperture photoconductor [1], which we call photoconducting antennas, are an effective source of electromagnetic radiation in the spectral range from 100 GHz to 1 THz. Recently we extend the concept of a single photoconducting antenna to an array of photoconducting antennas. When illuminated by a train of properly spaced ultrashort optical pulses, an array of short

photoconducting dipole antennas emits a sub-millimeter wave beam which can be electrically steered by varying the periodicity of the voltage bias applied to the individual antenna elements. By controlling the static bias voltage on each antenna element, we can vary the direction of the emitted radiation and produce a collimated submillimeter wave beam that is electrically steerable by a simple and effective technique.

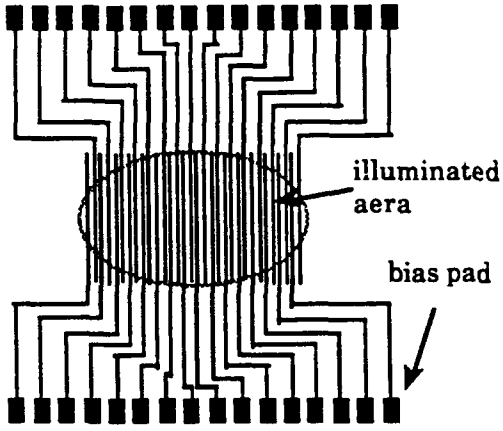

Fig. 7a: Top view of a 32-element photoconducting antenna array.

The array of photoconducting antennas is created by a pattern of parallel electrodes, each independently biased, on a semi-insulating GaAs substrate as illustrated in figure 7a. By setting the bias voltage on the electrodes appropriately, the amplitude of the photocurrent between every two adjacent electrodes can be controlled. When an optical pump pulse illuminates the structure, each current element acts roughly like a short dipole antenna. The far-field pattern of the array can be calculated according to conventional antenna theory [2] and is given by the approximate expression:

$$E(\theta) = \frac{A\cos\theta}{4\pi\varepsilon_0 c^2 r}\left[\frac{\mu e}{\hbar\omega}\right]\sum_{n=1}^{n=N}\left(\frac{V_n - V_{n-1}}{d}\right)I_n(\Omega)e^{-inKd\sin\theta} \quad (1)$$

where A is the optically illuminated area of the array, θ is the angle defined from the array normal, r is the radial distance, μ is the carrier mobility of the photoconductor, ω is the optical frequency, N is the number of electrodes under the illumination, V_n is the bias voltage on the nth electrode, d is the spacing between the photoconductor elements, $I_n(\Omega)$ is the optical intensity at the nth electrode, modulated at the microwave frequency Ω, and K is the

microwave free space propagation constant. If the strengths of the static bias voltage on each antenna element are made to vary periodically with respect to one another, the array will act like an amplitude grating, steering the beam in a direction which can be controlled by varying the bias period. Specifically, if the static bias voltages vary sinusoidally in space, with period Λ_{bias}, as:

$$V_n = \frac{E_0}{\kappa}\cos(n\kappa d) \qquad (2)$$

where Eo is the maximum static field between adjacent electrodes, $\kappa = (2\pi/\Lambda_{bias})$ and the optical intensity is uniform, then the radiated signal in the far-field can be approximated by the expression:

$$E(\theta) \approx \cos\theta\left[\frac{A\mu e E_0 I(\Omega)}{4\pi\varepsilon_0 c^2 r\hbar\omega}\right]\frac{\sin(Nd[\kappa \pm K\sin\theta])}{\sin(d[\kappa \pm K\sin\theta])} \qquad (3)$$

Four main lobes are expected, one pair inside and one pair outside the semiconductor. In free space, the maxima are at angles where $\sin\theta = \pm k/K$. Clearly, by varying the periodicity of the voltage bias, the emission angle of these lobes can be steered continuously over a range from zero to $\pm \pi/2$. The concept is illustrated in figure 7b.

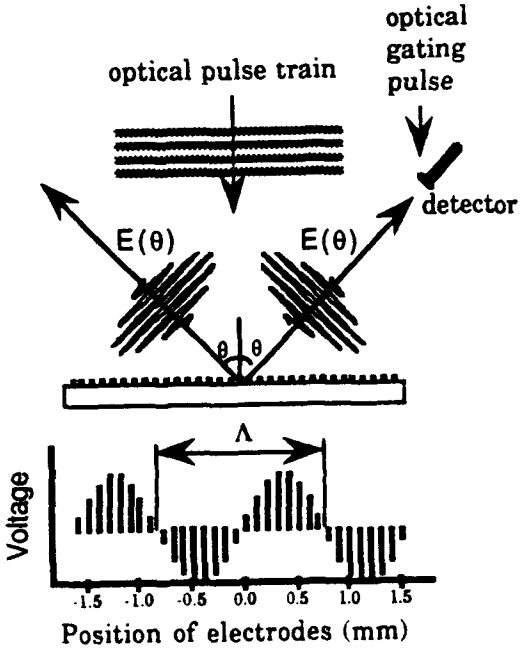

Fig. 7b: 500 GHz electromagnetic beam can be controlled by varying the spatial distribution of applied bias across the array.

Ideally, the temporal modulation on the optical illumination should be sinusoidal at the frequency of the emitted radiation. To approximate this condition, we have used a train of ultrashort optical pulses spaced by 2 ps to produce a burst at 500 GHz. A dual-jet, hybrid mode-locked dye laser, synchronously pumped at 78 MHz by a frequency-doubled YLF laser (Coherent Antares-Satori system), generated optical pulses at 640 nm with a duration of approximately 150 femtoseconds. The unfocussed beam, having a Gaussian profile 3 mm wide and an average power of 130 mW, was used to illuminate the antenna array. A train of four optical pulses of equal intensity, each spaced 2 psec apart, was generated by passing a single optical pulse through two calcite crystals having birefringent delays of two and four picoseconds.

The antenna array used in our experiments (figure 7a) consisted of 32 parallel electrodes, each 2 mm long and 25 microns wide, spaced 100 microns apart center to center. The electrodes, on a semi-insulating GaAs substrate, were made of gold germanium with a top layer of pure gold to facilitate wire bonding, giving a total thickness of about 2000 angstroms. The electrodes in the array were biased sinusoidally with respect to one another, as shown in figure 7b, using slide potentiometers so that the bias period could be easily varied. The voltages were scaled so that the maximum E field between elements was kept constant at 1.25 kV/cm for all bias periods, ensuring that the amplitude of the emitted radiation was constant. Due to the relatively low transient mobility of this material, we expect the photocurrent to be proportional to the product of the applied field and the absorbed optical flux.

The radiated field was detected with a photoconducting dipole antenna [3]. It consisted of a 100-μm dipole having a radiation-damaged silicon-on-sapphire photoconductor at its feed point. A 3 mm sapphire ball lens was placed over the dipole to improve its collection efficiency [4]. These antennas have a spectral response that peaks at 500 GHz and extends to 1 THz. The probe pulse had an average optical power of 10 mW and was focused to approximately 5 mm at the photoconductor in the dipole detector.

Radiated electric field waveforms were measured by using a correlation technique developed previously for studying other optoelectronic devices [3]. The field strength as a function of time was obtained by recording the gated output current from the dipole detector while varying the relative time delay between the pump pulses which illuminated the antenna array and probe pulse which gated the detector. The detected waveform at an angle of 45 degrees off normal and 3 cm from the array is shown in Figure 8. The periodicity of the voltage bias in this case was adjusted to be 0.9 mm to produce a maximum signal in the direction of the detector (equation 3). The 500 GHz burst is clearly resolved. Because the radiation from different antenna elements experiences different delay times, the emitted pulse train is broadened in time with respect to the optical pulse train.

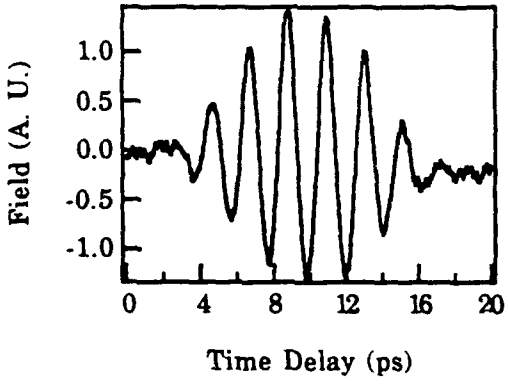

Fig. 8: Detected radiation waveform of a 500 GHz electromagnetic pulse burst from the array.

To test the steerable property of the array, the detector was kept fixed at 45° and the periodicity of the voltage bias was varied to sweep the angle of the emitted beam across the detector. The bias voltage amplitude was changed with period to maintain a constant maximum electric field, as in equation 2. The time traces obtained for each bias period were fourier transformed so that the signal amplitude at 500 GHz could be measured. The 500 GHz signal is plotted as a function of bias period in Figure 9. The signal peaks for a bias period close to the expected value. A theoretical curve of the variation in the signal is also plotted in Figure 9. It is based on the simple model of equation (1), assuming that the optical intensity profile is Gaussian. The width of the scanning beam at the 3 db points was

approximately 10°. This width is determined by the overall length of the array (3.2 mm) and could be much narrower if a larger array were used.

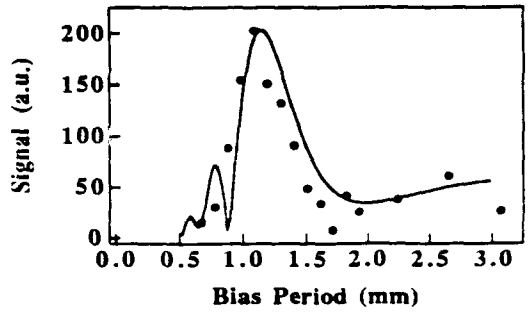

Fig. 9: The 500 GHz signal is plotted as a function of bias period

Measurements were also made using a single optical pulse to illuminate the array instead of a train of pulses. In this case the peak amplitude of the waveform did not fall off as rapidly as the period was changed, showing that the beam was less directional than the four-pulse case, as expected. Also, the spectrum of the emitted radiation varied strongly with angle due to the dispersive property of the periodic array.

Some variations on this basic device concept merit discussion. In our initial configuration, the optical illumination was at normal incidence to the array. This resulted in two beams being emitted in symmetric directions about the normal. By using non-normal incidence, the beams can be further steered off axis as we have previously demonstrated with large uniform photoconducting apertures [1]. This could be used to advantage to suppress one of the emitted beams. Using multiple pulse trains to produce a 100% modulated optical signal is an expedient that served well to illustrate the basic properties of this device. A more effective approach might be to mix two quasi-continuous optical pulses with carrier frequencies separated by a microwave frequency as in optical heterodyning experiments. 500 GHz was a convenient frequency for a first experiment. However, lower frequencies in the microwave band might prove to be more useful for applications. The emitted power in our experiment could be substantially increased by scaling the optical power, bias voltage, and array dimensions. Recent scaling experiments with uniformly biased large aperture photoconductors suggest that very high peak powers should be possible [5]. Possible applications for

this device are steerable radar systems and microwave sub-carrier demodulation for optical communications.

References:

[1] B.B. Hu, J.T. Darrow, X.-C. Zhang, and D.H. Auston, Appl. Phys. Lett. **56**, 886 (1990).

[2] J.D. Kraus, Antennas, second edition, Chapter 4, MaGraw Hill Book Co.

[3] P.R. Smith, D.H. Auston, and M.C. Nuss, IEEE J. Quantum Electron. **24**, 255 (1988).

[4] Ch. Fattinger and D. Grischkowsky, Appl. Phys. Lett. **54**, 490 (1989).

[5] J.T. Darrow, X.-C. Zhang, and D.H. Auston, Appl. Phys. Lett. **58**, 25 (1991).

c. Electrically Controlled Frequency Scanning by an Array.

Using a photoconducting antenna array, we can electrically scan the radiation frequency of an electromagnetic wave from a spatial periodically-biased photoconducting antenna array by varying the periodicity of the bias voltage on the antennas. Over 900 GHz frequency tuning bandwidth has been demonstrated.

Photoconducting antennas under the optical excitation of a single femtosecond laser pulse are an effective source of THz bandwidth electromagnetic radiation [1]. We have recently demonstrated that a photoconducting antenna array can electrically steer a 500 GHz electromagnetic wave in free space [2]. With a train of properly spaced ultrashort optical pulses illuminating on an array of short photoconducting dipole antennas, the array emits a sub-millimeter wave beam which can be electrically steered by varying the periodicity of the voltage bias applied to the individual antenna elements.

We have studied the frequency tuning property of the photoconducting antenna array. At a given angle, the radiation frequency of the optically induced electromagnetic wave from the array can be electrically tuned over a wide range. We have achieved a tuning range of the center frequency from 140 GHz to 1.06 THz. This tuning range can be used for the electronically-controlled synthesis of the submillimeter waves

in free space. The possible application of ultrahigh speed microwave or millimeter wave multiplexer / demultiplexer is discussed.

The antenna array has been previously used to electrically steer the electromagnetic radiation [2]. Basically, it consists of 32 parallel electrodes fabricated on a semi-insulating GaAs substrate. Each electrode is a 25 mm wide and 2 mm long Au microstrip transmission line. The photoconducting gap between the adjacent electrodes is 75 mm, making an array active window of 2x3.2 mm^2. Each electrode was individually biased. The spatial distribution of the bias amplitude on the electrodes was a sinusoidal function

$$V_n = \frac{E_0}{\kappa}\cos(n\kappa d + \phi) \tag{1}$$

where V_n is the voltage of the nth electrode, E_0 is the field, d is the space between adjacent electrodes and ϕ is the phase, and $k = (2p/\Lambda_{bias})$ where Λ_{bias} is the bias period. Typical value of the field E_0 was 12.5 kV/cm. Due to the spatial resolution imposed by using 32 electrodes, the bias period Λ_{bias} was only varied from 0.4 mm to 3.2 mm, corresponding to a change from 8 cycles to 1 cycle of the sinusoidal distribution across a 3.2 mm array, respectively.

A single optical pulse with a 150 fs pulse duration illuminated the array at a normal incident angle. The dipole detector was placed 30 mm away from the emitting array at a detection angle of q. At a given angle q, the far field radiation E(q) from a photoconducting antenna array with a sinusoidal distributed static voltage in space as described in equation (1) can be an approximately expressed as [2,4]:

$$E(\theta) \propto \cos\theta \frac{\sin(Nd[\kappa \pm K\sin\theta])}{\sin(d[\kappa \pm K\sin\theta])} \tag{2}$$

where N is the number of electrodes under the illumination, and K is the microwave free space propagation constant, which can be written as $K=(2\pi/\lambda)$ where λ is the center wavelength of the radiation. From equation (2), the maxima radiation are at the condition of $k=\pm K\sin\theta$. This condition can be rewritten as $\lambda=\pm\Lambda_{bias}\sin\theta$. It is clear that for a fixed angle θ, the

center wavelength λ is proportional to Λ_{bias}. Therefore by varying the bias period Λ_{bias}, the radiation wavelength λ (or radiation frequency f) can be electrically tuned at a defined direction.

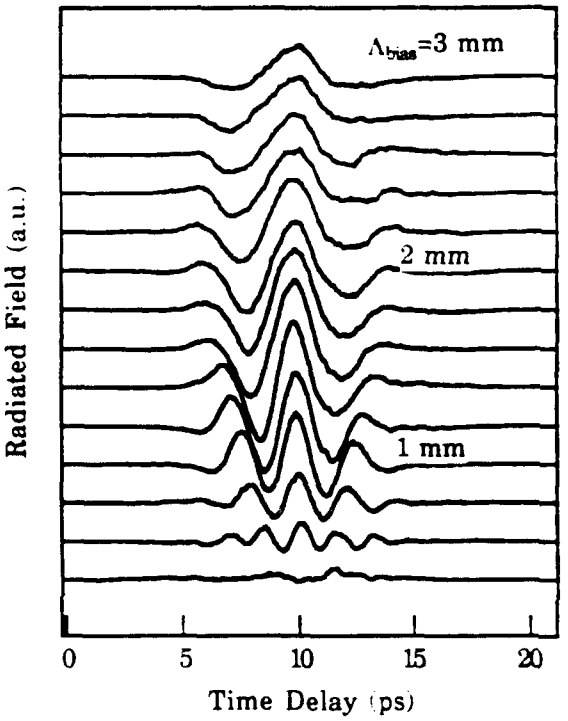

Fig. 10: Radiation waveforms vs bias period. The waveform reflects the spatial distribution of the bias field across the array.

To illustrate tuning properties of the photoconducting antenna array, we plot the temporal waveforms of the radiated fields versus the bias period Λ_{bias}, as shown in Figure 10. The number of the pulses in a wave packet is proportional to the number of the bias cycles. For a better vision, the curves have been offset. The bias period Λ_{bias} was varied from 0.4 mm to 3 mm and the No. 16 electrode was kept at the highest voltage. Since the center wavelength λ of the radiation is proportional to the bias period, increasing the bias period Λ_{bias}, causes the radiation wavelength to increase and the pulse width to broaden.

The temporal waveforms have been transformed into a frequency spectrum. The center carrier frequency of each waveform has been plotted versus the bias period Λ_{bias}, as shown in Figure 11. The solid dots are the measured values and the curve is the calculation from the equation $f=c(\Lambda_{bias}\sin\theta)^{-1}$. When the bias period increases from 0.4 mm to 3 mm, the main peak of the frequency decreases from 1.06 THz to 140 GHz. The

experimental data and the theoretical calculation are in good agreement. When the frequency was tuned over 1 THz, the measured amplitude of the radiation decreased, due to the frequency response of the dipole detector and the frequency response of the radiation from a single antenna. No radiated signal has been measured when the bias had linear distribution ($V_n=nE_0$). In this case, the radiation direction satisfies Fresnel's law [1]. The tuning bandwidth and resolution is largely determined by the size of the array and the number of the antennas. For an array size of 10x10 cm^2 with 50 mm photoconducting gaps, we expect that the tuning range can cover from 3 GHz to over 1 THz. The upper limit of tuning range is comparable with the bandwidth of radiation from a single antenna.

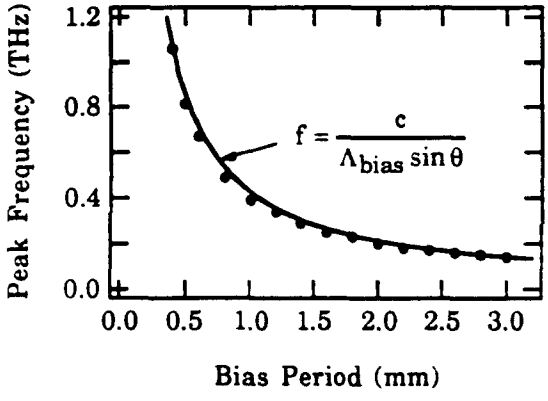

Fig. 11: Center frequency (peak) of the radiation field vs the bias period.

With an ultrafast optical pulse excitation (assuming the pulse width of the radiated field from a single antenna is much less than the array retardation time τ_a), the temporally spread radiation waveform reflects the spatial distribution of the bias across the array, because the radiation from different antenna elements experiences different delay times. For example, the voltage of the center electrode (No. 16) was kept at the highest value when the periodicity of the bias was changed, this caused the waveforms in Fig. 10 to have a symmetry near their centers (approximately at 10 ps position). Also when the bias phase f in equation (1) varied, pulses within the wave package shifted in time. The amount of the shift was $(\phi\sin\theta)/(ck)$. The direction of the shift depended on the sign of the phase ϕ, and the shift was confined within the duration of the array retardation time τ_a.

One possible application of this array is an ultrahigh speed microwave or millimeter wave time-division multiplexer / demultiplexer.

For a multiplexer, the information can be electronically encoded through the variation of the voltage profile on the parallel electrodes. Since the temporal radiation waveform carries the spatial bias distribution, as previously mentioned, the spatially input information should be timely recorded on the radiation waveform. To use an array as a demultiplexer, the operation is just the reverse of that of a multiplexer. If the spatial distribution of the bias across the array is a superposition of several sinusoidal functions, such an array can be further used as a wavelength-division multiplexer / demultiplexer.

References:

[1] B.B. Hu, J.T. Darrow, X.-C. Zhang, and D.H. Auston, Appl. Phys. Lett. **56**, 886 (1990).

[2] N. Froberg, M. Mack, B.B. Hu, X.-C. Zhang, and D. H. Auston, submitted to Appl. Phys. Lett., MS# L-8026 (1990).

[3] P.R. Smith, D.H. Auston, and M.C. Nuss, IEEE J. Quantum Electron. **24**, 255 (1988).

[4] J.D. Kraus, Antennas, second edition, Chapter 4, MaGraw Hill Book Co. (1988).

d. Carrier Dynamics with Photoexcitation Around Bandgap.

We have recently installed a Nd:YLF pumped dye laser system. This system, the Antares-Satori laser by Coherent Inc. produces a source of wavelength tunable femtosecond pulses. We have begun to use this system to do experiments in which we measure the optically-induced terahertz radiation from semiconductor surfaces as the optical excitation wavelength is tuned close to the band edge. We have been able to study the dynamics of the relaxation of the injected photocarriers when the wavelength of the optical excitation is near the semiconductor band-gap. Our preliminary experimental results show that a negative photocurrent can be formed when the excess energy of the injected photocarriers is equal to a multiple of one LO phonon energy. When the excitation was tuned below the semiconductor bandgap, we have also observed terahertz electromagnetic radiation due to the inverse Franz-Keldysh effect (virtual photoconductivity). All these measurements are extremely useful for understanding the transient carrier dynamics when the injected electron energy is selectively tuned by the variable wavelength optical excitation. This work is continuing and will be the subject of next year's research under the renewal of this grant.

C. PUBLICATIONS.

1. D.H. Auston, "Picosecond photoconductivity: High speed measurements of devices and materials," to be published as a chapter of the book: *Probing high speed electrical signals* , edited by R. B. Marcus, Academic Press, (1989).

2. D.H. Auston, "Probing semiconductors with femtosecond pulses", Physics Today, February , 46-54, (1990).

3. B.B Hu, X.-C. Zhang, D.H. Auston and P.R. Smith, "Free Space Radiation from Electro-Optic Crystal," Appl. Phys. Lett. **56**, 506 (1990).

4. B.B Hu, J.T. Darrow, X.-C. Zhang, D.H. Auston and P.R. Smith, "Optically-Steerable Photoconducting Antennas," Appl. Phys. Lett. **56**, 886 (1990).

5. X.-C. Zhang, B.B Hu, J.T. Darrow and D.H. Auston, "Generation of Femtosecond Electromagnetic Pulses from Semiconductor Surfaces," Appl. Phys. Lett. **56**, 1011 (1990).

6. J.T. Darrow, B.B Hu, X.-C. Zhang and D.H. Auston, "Subpicosecond Electromagnetic Pulses from Large Aperture Photoconducting Antennas," Opt. Lett., **15**, 323 (1990).

7. X.-C. Zhang, J.T. Darrow, B.B. Hu, D.H. Auston, M.T. Schmidt, P. Tham and E.S. Yang, "Optically Induced Electromagnetic Radiation from Semiconductor Surfaces," Appl. Phys. Lett. **56**, 2228 (1990).

8. C. Shu, B.B. Hu, X.-C. Zhang, P. Mei, and E.S. Yang, "Picosecond Photoconductive Response of Polycrystalline Silicon Thin Films," Appl. Phys. Lett. **57**, 64 (1990).

9. X.-C. Zhang, B.B Hu, X.H. Xin and D.H. Auston, "Optically Induced Femtosecond Electromagnetic Pulses from GaSb/AlSb Strained Layer Superlattices," Appl. Phys. Lett. **57**, 753, (1990).

10. B.B. Hu, X.-C. Zhang, and D.H. Auston, "Temperature Dependence of Optically Induced Femtosecond Electromagnetic Radiation from Semiconductor Surfaces," Appl. Phys. Lett. **57**, 2629 (1990).

11. X.-C. Zhang, B.B. Hu, J.T. Darrow, S.H. Xin and D.H. Auston, "Optical Measurement of Piezoelectric Field in Strained Layer Superlattices," submitted to Opt. Lett. (1990).

12. X.-C. Zhang, J.T. Darrow, B.B. Hu, S.H. Xin and D.H. Auston, "Optically Induced Electromagnetic Radiation from Semiconductor Surfaces," Spring Series in Chemical Physics, **53**, 198 (1990).

13. C. Shu, X.-C. Zhang, E.S. Yang and D.H. Auston, "Generation and Propagation of Optoelectronic Signals in Coplanar Waveguides,"Appl. Phys. Lett. **57**, 2897 (1990).

14. C. Shu, X.-C. Zhang, E.S. Yang and D.H. Auston, "Optoelectronic Generation and Detection of 80 Gbit/s Pulse Train," IEDM Tech. Digest , 327 (1990).

15. J.T. Darrow, X.-C. Zhang and D.H. Auston, "Power Scaling of Large-Aperture Photoconducting Antennas," Appl. Phys. Lett. **58**, 25 (1991).

16. N. Froberg, M. Mack, B.B. Hu, X.-C. Zhang and D.H. Auston, "500 GHz Electrically-Steerable Photoconducting Antenna Array," App. Phys. Lett. **58**, 446 (1991).

17. B.B. Hu, N. Froberg, M. Mack, X.-C Zhang and D.H. Auston, "Electronically-controlled Frequency Scanning by Photoconducting Antenna Array," App. Phys. Lett. **58**, 1369, (1991).

18. L. Xu, X.-C. Zhang, D.H. Auston and W.I. Wang, "Internal Piezoelectric Field in Strained Layer GaInSb/InAs Superlattices Probed by Optically Induced Microwave Radiation," submitted to Appl. Phys. Lett, (1991).

19. C. Shu, X. Wu, E.S. Yang, X.-C. Zhang and D.H. Auston, "Propagation Characteristics of Picosecond Electrical Pulses on a Periodically Loaded Coplanar Waveguide," IEEE Trans. Microwave Theory Tech. MTT-**39**, 930 (1991).

20. X.-C. Zhang and D.H. Auston, "Generation of Steerable Submillimeter-Waves from Semiconductor Surfaces by Spatial Light Modulators," Appl. Phys. Lett., **59**, 768 (1991).

21. D.H. Auston and X.-C. Zhang, "Larger Aperture Photoconducting Antennas," Picosecond Electronics and Optoelectronics VI, Springer Series in Electronics and Photonics, (1991).

22. X.-C. Zhang and D.H. Auston, "Optically Induced THz Electromagnetic Radiation from Planar Photoconductive Antennas," to be publised in JEWA, (1991).

23. X.-C. Zhang and D.H. Auston, "Optoelectronic Characterization of Semiconductor Surfaces and Interfaces with Femtosecond Optics," to be publised in J. Appl. Phys., (1991).

24. L. Xu, X.-C. Zhang and D.H. Auston, "Transition Radiation from Femtosecond Optical Pulses in Electro-optic Materials," to be submitted to Appl. Phys. Lett., (1991).

25. N. Froberg, B.B. Hu, X.-C. Zhang and D.H. Auston, "Time-division Multiplexing Performed by A Photoconducting Antenna Array," submitted to Appl. Phys. Lett. (1991).

26. B.B. Hu, X.-C. Zhang and D.H. Auston, "Observation of Negative Photo-conductivity in GaAs," to be submitted to Phys. Rev. B. (1991).

27. P.M. Ferm, C. Knapp, C.-J. Wu, J.T. Yardley, B.B. Hu, X.-C. Zhang and D.H. Auston, "Ultrafast Electrooptic Effect in Poled Polymer Films," to be publised in Appl. Phys. Lett. (1991).

28. J.T. Darrow, X.-C. Zhang and D.H. Auston, "Saturation Properties of Large-Aperture Photoconductor Antennas," submitted to IEEE JQE. (1991).

29. D.C. MacPherson, A.J. Taylor, N.A. Kurnit, X.-C. Zhang and D.H. Auston, "Theory of Electromagnetic Pulse Generation Using Photoconducting Switches," to be submitted to IEEE JQE (1991).

30. B.B. Hu, X.-C. Zhang and D.H. Auston, "Terahertz Radiation Induced by Subbandgap Femtosecond Optical Excitation of GaAs," submitted to Phys. Rev. Lett. (1991).

31. Li Xu, A. Hasegawa and D. H. Auston, "Propagation of Electromagnetic Solitary Waves in Dispersive Nonlinear Dielectrics", to be published in Phys. Rev. A (1991).

D. PERSONNEL.

The following personnel are currently supported by this contract:

Research Scientist: X.-C. Zhang, 6 months salary support.

Ph.D Students: B. B. Hu and L. Xu.

E. INTERACTIONS.

1. *Conference Presentations and Seminars:*

[1] "Characterization of Semiconductor Surfaces by Femtosecond Optical Rectification", International Quantum Electronics Conferences, Anaheim, May 22, 1990.

[2] "Large Aperture Photoconducting Antennas," Conference on Laser and Electro-Optics, Anaheim, May 22, 1990.

[3] "Optically Induced Electromagnetic Pulses from Semiconductor Surfaces", Topical Meeting of Ultrafast Phenomena, Monterey, May 16, 1990.

[4] "Generation of Ultrafast Electromagnetic Radiation," Optical Society of America Annual Meeting, Boston, Nov. 4, 1990.

[5] "Generation and Detection of Ultrafast Pulsed Electromagnetic Radiation by Large-Aperture Photoconducting Antennas," Optical Society of America Annual Meeting, Boston, Nov. 4, 1990.

[6] "Optical Characterization of Piezoelectric Fields in Strained-Layer Superlattices", Optical Society of America Annual Meeting, Boston, Nov. 4, 1990.

[7] Conference on Lasers and Electro-Optics, Opt. Soc. Amer., Washington, D.C., 1990.*

[8] "Electrically-steered Photoconducting Antenna Array," Optical Society of America Annual Meeting, Boston, Nov. 4, 1990.

[9] "Femtosecond Electromagnetic Radiation from Semiconductor Surfaces," Workshop on the Optically Controlled Phased-Array Antennas, University of South California, Oct. 15, 1990.

[10] "Optoelectronic Generation and Detection of 80 GBit/s Pulse Train," International Electron Devices Meeting, San Francisco, Jan. 11, (1991)

[11] "Large Aperture Photoconducting Antennas," Topical Meeting of Picosecond Electronics and Optoelectronics, Salt Lake City, Mar. 13, 1991.

[12] "Large Aperture Photoconductive Antennas and Antenna Arrays," High Speed/High Frequency Optoelectronics Conference , Palm Coast, Mar. 21, 1991.*

[13] "Saturation Properties of Large-aperture Photoconducting Antennas," Conference on Laser and Electro-optics, Baltimore, May 17, 1991.

[14] "Electrically-controlled Pulse Shaping and Frequency Scanning of Terahertz Submillimeter Waves," Conference on Laser and Electro-optics, Baltimore, May 17, 1991.

[15] "Directionality of Terahertz Electromagnetic Waves From Photoconducting Antenna Arrays," Conference on Laser and Electro-optics, Baltimore, May 17, 1991.

[16] "Observation of Negative Transient Photoconductivity In GaAs," Quantum Electronics and Laser Science Conference, Baltimore, May 17, 1991.

[17] "Steerable THz Radiation from Photoconductor Arrays," Workshop on the Optically Controlled Phased-Array Antennas, University of South California, June. 15, 1990.

[18] "Optically Induced THz Electromagnetic Radiation From Planar Photoconducting Structures", Progress in Electromagnetic Research Symposium, Boston, Jul. 3, 1991.

[19] "Generation of Submillimeter-wave Pulses From Surfaces With Femtosecond Optics," LEOS Summer Topical Meeting On Optical Millimeter-wave Interaction: Measurements, Generation, Transmission and Control, Newport Beach, Jul. 25, 1991.

2. *Consulting & Advisory Activities.*

Member of the Research Board of Hewlett Packard Laboratories.
Special Consultant and member of the External Advisory Board for Optics Research and Development of the Eastman Kodak Company.
Consultant to AT&T Bell Laboratories.
Member of the Scientific Advisory Board, NSF Engineering Research Center for Optoelectronic Computing Systems, University of Colorado.
Member of the Scientific Advisory Board, Center for High Technology Materials, University of New Mexico.
Member of the Scientific Advisory Board, Ultrafast Optics Institute, City College, New York.

F. PATENTS.

"Source of Directional Electromagnetic Radiation," D. H. Auston and X.-C. Zhang. Patent pending.

"Noncontacting probing of semiconductor surfaces with femtosecond optical pulses," D. H. Auston and X.-C. Zhang. Patent disclosure.

"Generation of Steerable Terahertz Electromagnetic-Waves by Spatial Light Modulator," D.H. Auston and X.-C. Zhang. Patent pending.